Near field impulsive source localization in a noisy environment

Young-Chul Choi[a,*], Yang-Hann Kim[b]

[a]Advanced Reactor Tech. Korea Atomic Energy Research Institute (KAERI), 150 Duckjin-dong Yuseong-gu, Daejeon-shi, Republic of Korea
[b]Center for Noise and Vibration Control (NOVIC), Department of Mechanical Engineering,
Korea Advanced Institute of Science and Technology (KAIST), 373-1,Guseong-dong, Yuseong-gu, Daejeon, Republic of Korea

Abstract

When a machine has faults in its rotating parts, it normally generates a periodic vibration or acoustic signals. These signals are often periodic but impulsive. This paper addresses the way in which we can find out where the impulsive sources are. We propose a signal processing method that can identify an impulsive sources' location. The method is robust with respect to noise; a spatially distributed noise. Numerical simulation and experiments are performed to verify the method. Results show that the proposed technique is quite powerful for localizing the sources in noisy environments. The method also required less microphones than the conventional beamforming method.
© 2007 Elsevier Ltd. All rights reserved.

1. Introduction

In a previous study, the impulsive source was detected in a noisy environment to find the faults in a rotating machine at an early stage. McFadden and Smith [1] used the bandpass filter to filter the noise signal and then obtained the envelope by using an envelope detector. Lee and White [2] used improved an adaptive noise cancellation (ANC) to find faults. The basic idea of this technique is to remove the noise from the measured vibration signal. Kim et al. proposed a moving window [3] and Staszewski and Tomlinson [4] applied it to a tooth fault detection in gear boxes. However, these methods can find an impulse, only if the candidate location of the fault is known. In other words, they cannot estimate an impulsive source's location when there are many candidate sources in a space. Therefore, the method of localizing the impulse sources distributed in a space is needed.

Possible methods of these kinds can be classified into two cases. One is what is that based on a differential time delay estimation [5–7], the other is that utilizing a microphone array such as the beamforming method and an acoustic holography [8–13].

In fact, it is almost impossible to locate the impulsive source [18–24] in a factory with lots of reflections and to observe the impulse owing to the mechanical noise even in an anechoic chamber. This study is undertaken to present the method available for the latter situation; how to estimate the spatial location of an impulsive source in a noise. Under this method, the minimum variance method [11–14] with a high pulse detection ability was applied to the quefrency domain and used to find the impulsive sources' location using the beamforming method.

*Corresponding author. Tel.: +82 42 868 4870; fax: +82 42 868 8313.
E-mail address: cyc@kaeri.re.kr (Y.-C. Choi).

Therefore, this paper addresses the way in which we find the impulsive sources' location using beamforming method in the quefrency domain. Especially, we are interested in finding their locations when the signals are embedded in noise.

2. Impulsive source localization

The definition of an impulse noise varies from country to country and there is still no consistent definition. A recent recommendation from the International Standard Organization ISO2204 stated that an impulse noise can be characterized as a burst sound or continuous burst sounds with a duration time less than 1 s [15]. This indicates that an impulse noise is produced within the time interval mentioned above, therefore an adjustment is necessary to find the equivalent sound pressure level. On the other hand, IEC argued that an impulse noise can be a single-pulse sound or a burst sound with a duration time between 0.001 and 1 s [16].

In real-life situations, impulse noises are often heard from a variety of sources and in combination with one anothers. For example, if a machine has faults, it generates a signal that is usually composed of impulse signals. In addition, a noise source can be classified according to distance between the noise source and the receiver. A near field noise source identification of them has a great significance in mechanical engineering. Therefore, source identification in the presence of a spherical wave front must be studied.

In this paper, we deal with periodic impulsive source as shown in Fig. 1(b), the measured pressure $p(r, t)$ can be modeled as

$$p(r, t) = \frac{1}{r} h(t) \sum_{m=0}^{M} \delta\left(t - \frac{r}{c} - mT\right), \tag{1}$$

where r is the distance between the impulsive source and the microphone, $h(t)$ the system's impulse response function, M the number of impulses in a measured signal, c the wave speed, δ the Dirac delta function and T the period of the pulse train. As shown in Fig. 2(b), the signal from microphones 1 and 2 is represented by the following equations:

$$p_1(r_1, t) = \frac{1}{r_1} h(t) \sum_{m=0}^{M} \delta\left(t - \frac{r_1}{c} - mT\right),$$

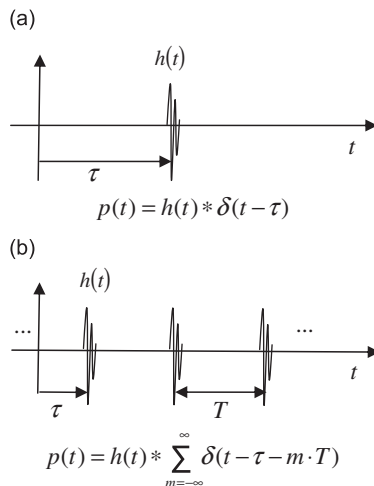$$p_2(r_2, t) = \frac{1}{r_2} h(t) \sum_{m=0}^{M} \delta\left(t - \frac{r_2}{c} - mT\right), \tag{2}$$

Fig. 1. Impulse noise can be characterized as a bust sound or continuous burst sound with a duration time less than 1 s [2], for example (a) an impulse noise, (b) continuous impulse noise (impulse train). In this study, we are interested in both an impulse noise and an impulse noise train.
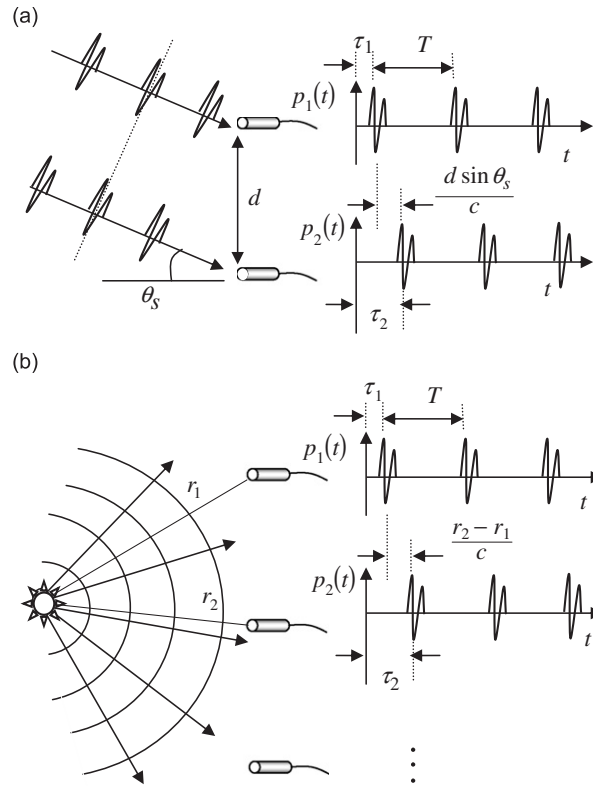
Fig. 2. (a) Impulsive source localization in the plane wave model. (b) Spherical wave model. Where d is the microphone spacing, c is the wave speed, θ_s is the direction of the noise sources, T is the impulse noise period and r_i is the distance between the ith microphone and the impulse sources.

where r_i is the distance between the source location and the ith microphone. The Fourier transform of $p(r, t)$ leads to

$$P_1(r_1, \omega) = \frac{1}{r_1} H(\omega) e^{j\omega(r_1/c)} \sum_{m=0}^{M} e^{j\omega mT},$$

$$P_2(r_2, \omega) = \frac{1}{r_2} H(\omega) e^{j\omega(r_2/c)} \sum_{m=0}^{M} e^{j\omega mT}, \tag{3}$$

where $H(\omega)$ is the Fourier transform of $h(t)$. The ratio between $P_1(\omega)$ and $P_2(\omega)$ can be readily obtained from Eq. (3), that is

$$\frac{P_2(r_2, \omega)}{P_1(r_1, \omega)} = \frac{r_1}{r_2} e^{j\omega((r_2-r_1)/c)}. \tag{4}$$

In the frequency domain, the transfer function between the two microphones is represented as a sinusoidal function with a period, which is the impulse time delay between the two microphones.

If the impulsive signal embedded in noise, Eq. (4) can be replaced with (see detailed derivation in Appendix A)

$$\frac{P_2(r_2, \omega)}{P_1(r_1, \omega)} = \frac{r_1}{r_2} e^{j\omega((r_2-r_1)/c)} + N(\omega). \tag{5}$$

Eq. (5) means that the sinusoidal signal is embedded in noise in the frequency domain. It is noteworthy that we can detect the time domain sinusoidal signal in noise. This means we can obtain the sinusoidal function in Eq. (5); therefore impulsive source locations can be found.

In 1969, Capon coined a maximum likelihood [11] spectrum which estimates a mixed spectrum consisting of a line spectrum, corresponding to a deterministic random process, plus an arbitrary unknown continuous spectrum. The unique feature of this spectrum is that it can detect a sinusoidal signal embedded in noise. Therefore, we attempted to apply this method to Eq. (5).

Autocorrelation function $r(k)$ of Eq. (5) is

$$r(k) = \left| \frac{r_1}{r_2} \right|^2 e^{jk((r_2 - r_1)/c)} + \xi^2 \delta(k) \tag{6}$$

and the autocorrelation matrix $\mathbf{R}_S$ leads to [17]

$$\mathbf{R}_S = \left(\frac{r_1}{r_2} \right)^2 \mathbf{e}_S \mathbf{e}_S^H + \xi^2 \mathbf{I}, \tag{7}$$

where $\mathbf{e} = [1, \quad e^{j((r_2 - r_1)/c)} \quad \cdots \quad e^{jp((r_2 - r_1)/c)}]^T$, ξ^2 is the variance of $N(\omega)$, p the order of the bandpass lifter, and $\mathbf{I}$ means the identity matrix. Using Woodbury's identity [26], it follows that the inverse of $\mathbf{R}_S$ is

$$\mathbf{R}_S^{-1} = \frac{1}{\xi^2} \mathbf{I} - \frac{(1/\xi^4)\mathbf{e}_S \mathbf{e}_S^H}{1 + (1/\xi^2)\mathbf{e}_S^H \mathbf{e}_S} = \frac{1}{\xi^2} \left[\mathbf{I} - \frac{\mathbf{e}_S \mathbf{e}_S^H}{\xi^2 + (p+1)} \right]. \tag{8}$$

Since the definition of the minimum variance power [11,12] is $F_{MV}(\omega) = 1/\mathbf{e}^H \mathbf{R}_S^{-1} \mathbf{e}$, we can obtain the minimum variance power in the cepstrum domain where the impulse signal can be distinguished from noise:

$$
\begin{aligned}
F_{MV}(\tau) &= \frac{1}{\mathbf{e}^H \mathbf{R}_S^{-1} \mathbf{e}} \\
&= \frac{(\xi^2/(1+p)) + (r_1/r_2)^2}{1 + (r_1/r_2)^2 (1/\xi^2(1+p)) \left\{ (1+p)^2 - \left| \sum_{k=0}^{p} e^{jk\left\{ \tau - ((r_2' - r_1')/c) \right\}} \right|^2 \right\}}.
\end{aligned} \tag{9}
$$

Since the impulse signal can be distinguished from noise, F_{MV} represents the arrival time difference between the two microphones and the magnitude of F_{MV} is the signal power in the quefrency domain.

As shown in Fig. 2 and Eq. (4), the time difference of the impulse noise among the microphones is the most important one for a source identification. This is because the time difference is directly related to the location of the impulsive sources. Therefore, scan vector has to be

$$W_{ij}(\tau) = \delta\left(\tau - \frac{r_j - r_i}{c} \right), \tag{10}$$

where r_i is the distance between the scan impulse source and the ith microphone. Let us define the beamforming power in the τ domain as

$$P_{\text{beam}} = \int_{-\infty}^{\infty} F_{MV}(\tau) W(\tau) \, d\tau. \tag{11}$$

Eqs. (9)–(11) create our modified beamforming power, that is

$$P_{\text{beam}}(x, y, z) = \frac{\xi^2/(1+p) + (r_1/r_2)^2}{1 + (r_1/r_2)^2 1/(\xi^2(1+p)) \left\{ (1+p)^2 - \left| \sum_{k=0}^{p} e^{jk(1/c)\left\{ (r_2 - r_1) - (r_2' - r_1') \right\}} \right|^2 \right\}}, \tag{12}$$

where r_i' is the distance between the ith microphone and the true impulse source. $\sum_{k=0}^{p} e^{jk(1/c)\{(r_2 - r_1) - (r_2' - r_1')\}}$ is the discrete Fourier transform of a rectangular window that extends from $k = 0$ to p, the value of $|\sum_{k=0}^{p} e^{jk(1/c)\{(r_2 - r_1) - (r_2' - r_1')\}}|^2$ goes to $(p+1)^2$ when $r_2 - r_1 = r_2' - r_1'$ and $p \gg 1$. If $r_2 - r_1$ is not equal to $r_2' - r_1'$,
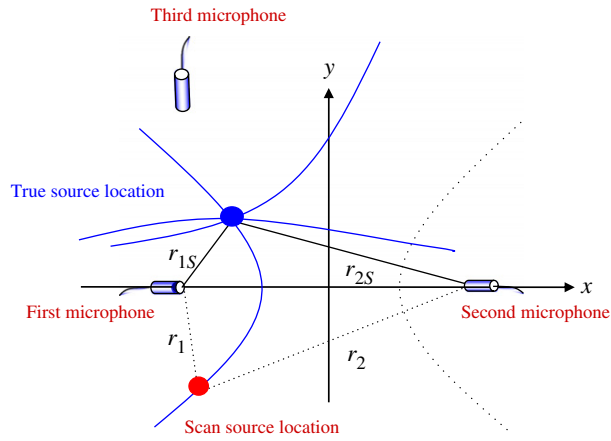
Fig. 3. Impulsive source localization for a two-dimensional space, where r_1 is the distance between scan source and i-th microphone, and r_{1s} is the distance between true source and i-th microphone.
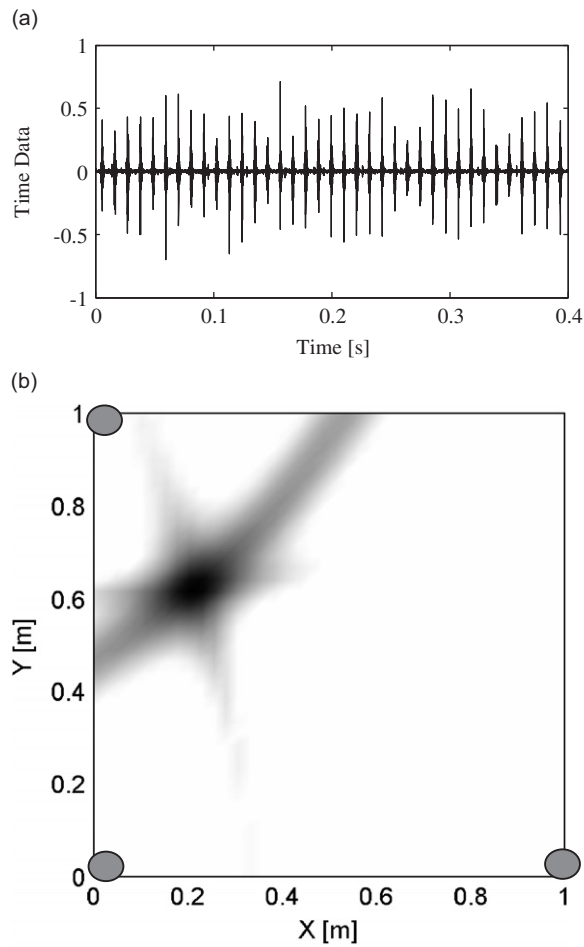

Fig. 4. Numerical simulation without a noise. The circle ⬤ means the microphone locations. The locations of the microphones are $(x, y) = (0\,\text{m}, 0\,\text{m})$, $(1\,\text{m}, 0\,\text{m})$, and $(1\,\text{m}, 0\,\text{m})$. (a) source signal whose location is $(x, y) = (0.2\,\text{m}, 0.6\,\text{m})$, (b) the result of impulsive source localization.
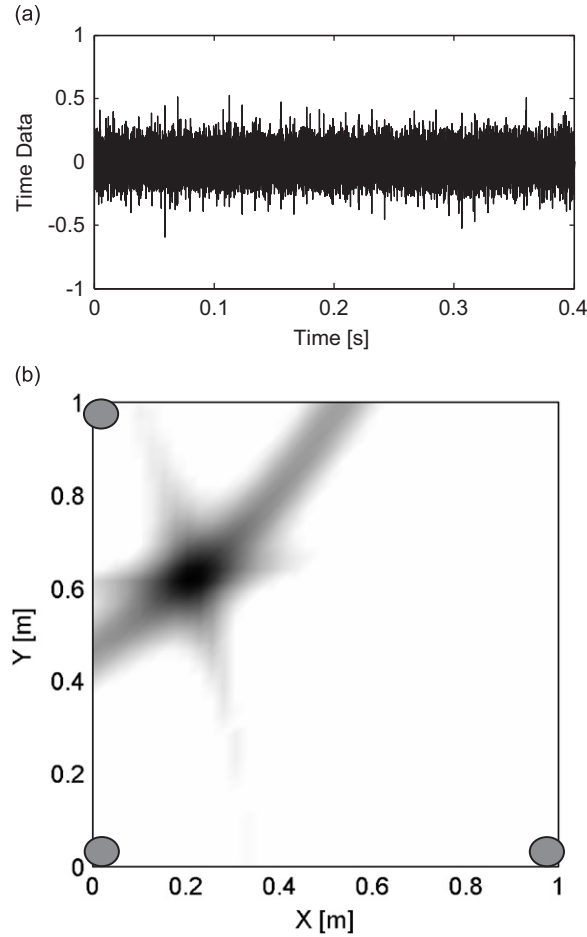
Fig. 5. Numerical simulation with a noise (signal-to-noise ratio $= 0.01$ and peak signal-to-noise ratio $= 0.8$). The circle ⬤ means the microphone locations. The locations of the microphones are $(x, y) = (0, 0)$, $(1, 0)$, and $(1, 0)$ (a) source signal whose location is $(x, y) = (0.2\,\text{m}, 0.6\,\text{m})$, (b) the result of impulsive source localization.

the value is near to zero. Therefore, Eq. (12) can be simply rewritten as

$$P_{\text{beam}}(x, y, z) = \begin{cases} \dfrac{\xi^2}{1+p} + \left(\dfrac{r_1}{r_2}\right)^2 & \text{for } r_2 - r_1 = r_2' - r_1', \\ \dfrac{\xi^2}{1+p} & \text{for otherwise.} \end{cases} \tag{13}$$

It is worthnoting that $\xi^2/(1+p)$ in Eq. (13) decreases as p increases at the location of $r_2 - r_1 = r_2' - r_1'$. Therefore, the magnitude of the beamforming power converges to $(r_1/r_2)^2$. However, when $r_2 - r_1$ is not equal to $r_2' - r_1'$, then the beamforming power decreases as p increases and finally it goes to zero. This is because as the bandwidth decreases a lesser noise power passes the filter. This allows us to find the locations of impulse signals, regardless of noise power.

The equation $r_2 - r_1 = r_2' - r_1'$ means that a set of all the points is at a constant difference between the impulsive source and the two microphones. That is, it coincides with the parabola definition. Therefore, to localize the impulsive source in a two-dimensional (2-D) space, another microphone is needed and then we can obtain the location of the impulsive source as shown in Fig. 3.

For a plane wave model, for example, where an impulsive noises' source is in a duct, we can easily find the location of impulsive source using only two microphones (see Eqs. (9) and (10)). However, more microphones

Fig. 6. The experimental setup for the automobile engine to identify the impulse noise source. Sampling frequency is 32.8 kHz, the number of microphones is 28 and the total length of time is 5.5 s: (a) Front side, (b) upper side, (c) right-hand side, and (d) left-hand side of the engine.

are necessary to obtain the source location if we are interested in the sound field in general. For example, a minimum 3 microphones are needed to identify impulsive sources in a 2-D space. Similarly, in a three-dimensional (3-D) space, at least 4 microphones must be used. Fig. 2 (b) shows a typical spherical wave front and a measured signal using microphones. Therefore, the modified beamforming power must be rewritten as

$$P_{\text{beam}} = \int_{-\infty}^{\infty} \sum_{i=1}^{N} \sum_{j=1}^{N} F_{\text{MV}(ij)}(\tau) W(\tau)\, d\tau,$$

$$= \int_{-\infty}^{\infty} \sum_{i=1}^{N} \sum_{j=1}^{N} F_{\text{MV}(ij)}(\tau) \delta\left(\tau - \frac{r_j - r_i}{c}\right) d\tau, \tag{14}$$

where $F_{\text{MV}(ij)}(\tau)$ means the time difference of the impulse noise between the ith and jth microphones, N is the number of microphones, and r_i represents the distance between the image source and the ith microphone.

3. Numerical simulation and experiments

To verify the proposed method, we have performed a numerical simulation. Fig. 4(a) shows the signal from the source. To identify the impulsive sources, we used 3 microphones whose locations were $(x, y) = (0\,\text{m}, 0\,\text{m})$,
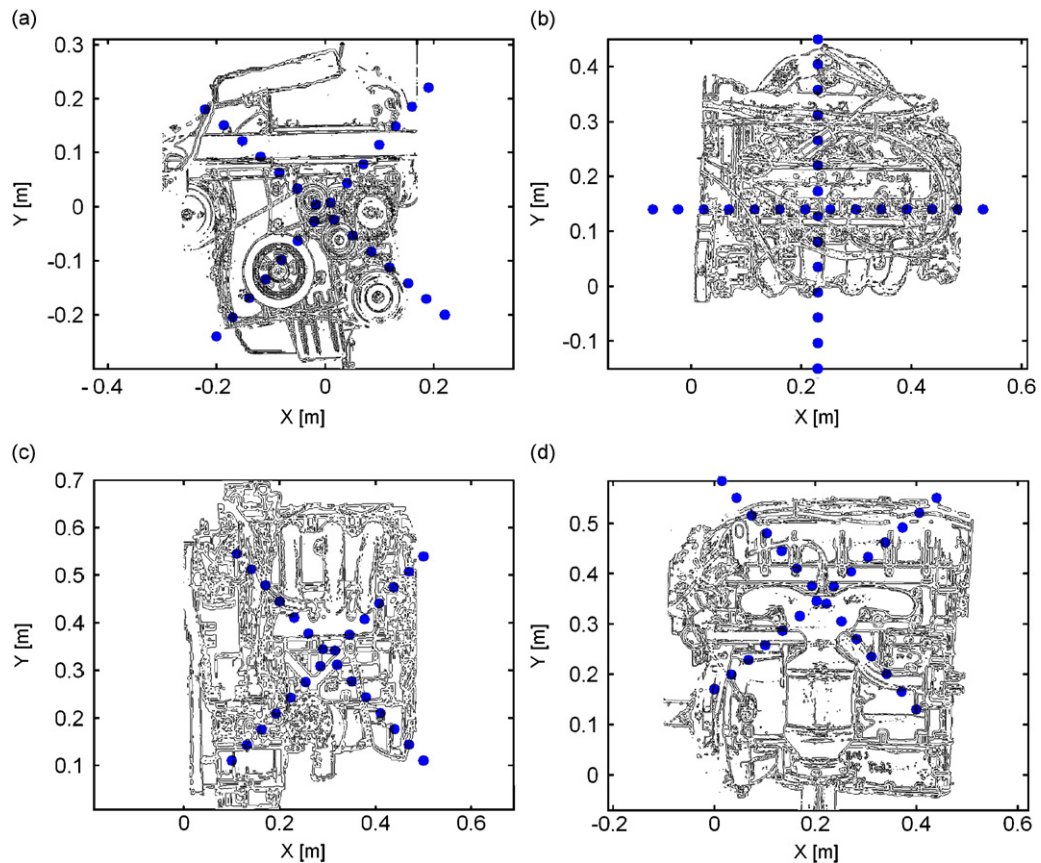
Fig. 7. The location of the microphone array. Sampling frequency is 32.8 kHz, the number of microphones is 28 and total length of time is 5.5 s: (a) front side, (b) upper side, (c) right-hand side, and (d) left-hand side of the engine.

(1 m, 0 m), and (0 m, 1 m). The signals obtained from microphones are produced by a convolution with transfer functions between the sources and the microphones in air. Fig. 4(b) shows the simulation results for localizing the impulsive source. We can examine that the beamforming powers have a maximum value at the location of the impulsive source. We can observe 3 parabolas whose origins are each microphone. The point of the crossing of the 3 parabolas is the impulsive source location. This is because the proposed method utilized the time delays of the impulsive signal to find the source location.

Fig. 5 demonstrates how powerful the method we proposed is, regardless of the signal to noise ratio. The signal from the microphone is artificially mixed with a white noise which has a Gaussian distribution (signal-to-noise ratio is 0.01 and peak signal to noise ratio is 0.08). As shown in Fig. 5(a), we could not find the impulse from the original time data. However, the impulsive source' location can be found using the proposed method as shown in Fig. 5(b). This numerical simulation demonstrates that the proposed method is able to find the location of the impulsive source in a noisy environment. It is independent of the level of noise as the theory proved. Also, it uses lesser microphones than the conventional beamforming method.

Fig. 6 essentially demonstrates the method's practical value. Fig. 6 shows the experimental setup for an automotive engine to identify impulse source. Sampling frequency is 32.8 kHz, and total time length is 5.5 s. We have used 28 microphones whose location are showed in Fig. 7. Fig. 8(a) shows the measured signal, which does not reveal a periodic impact signal and Fig. 8(b) shows the result of the minimum variance cepstrum. We cannot examine the impulsive noise in the original signal, but the result of minimum variance cepstrum shows the period of impulse train. This means that impulse train is embedded in noise. As we can imagine, it is not
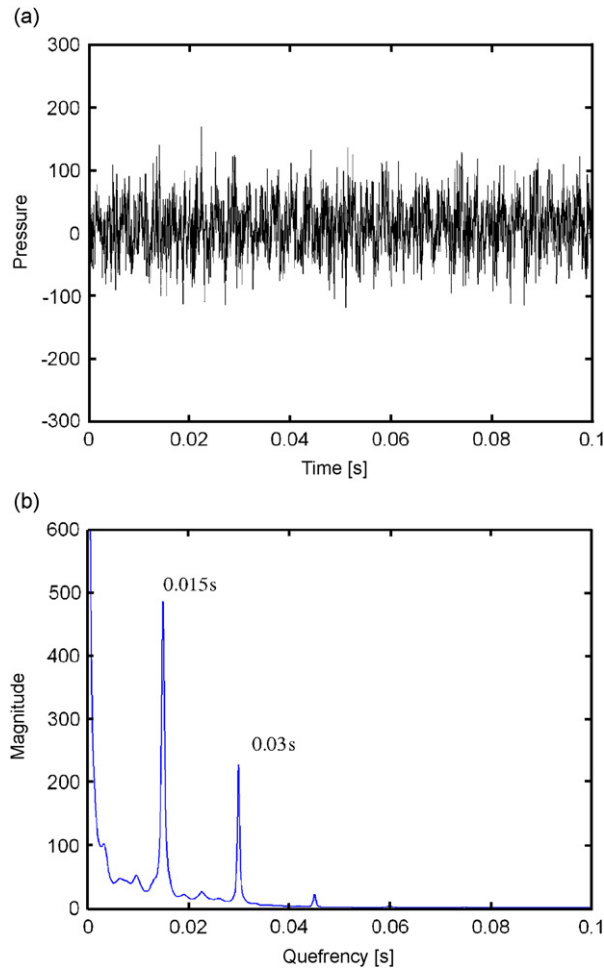
Fig. 8. (a) Measured pressure that does not show the impulse signal. (b) The result of the minimum variance cepstrum [14], which is a powerful signal processing for an impulse detection in a noise. The result shows that the measured signal has the impulse train with 0.015 s period.

just possible to recognize that there are impulsive noise in the engine we selected (Fig. 8(b)). However, in spite of the low signal to noise ratio, the method provides us with the location of impulsive source in an automobile engine as shown in Fig. 9. We can conclude that the main impulsive source is a valve train which produces impulsive noise!

4. Conclusions

We have introduced a signal processing that can effectively find the locations of impulsive sources embedded in noise. Theoretical formulation exhibits that the proposed method is independent of how much noise is embedded in the measured signal. If a sinusoidal signal and the noise properties are used in the quefrency domain, it would be easy to detect the impulsive source mixed with noise in the quefrency domain. Computer simulation was used to verify the presented method. It was found that it was easy to find exactly the location of the impulsive source in noise. Likewise, the same test was carried out for an automotive engine. Actually, it is difficult to observe the impulse under the semi-anechoic environment or lots of noises. The test for the automotive engine was carried out to detect the impulsive noises around the valves. In conclusion, the method in this study is very useful in locating an impulsive source under lots of noises.
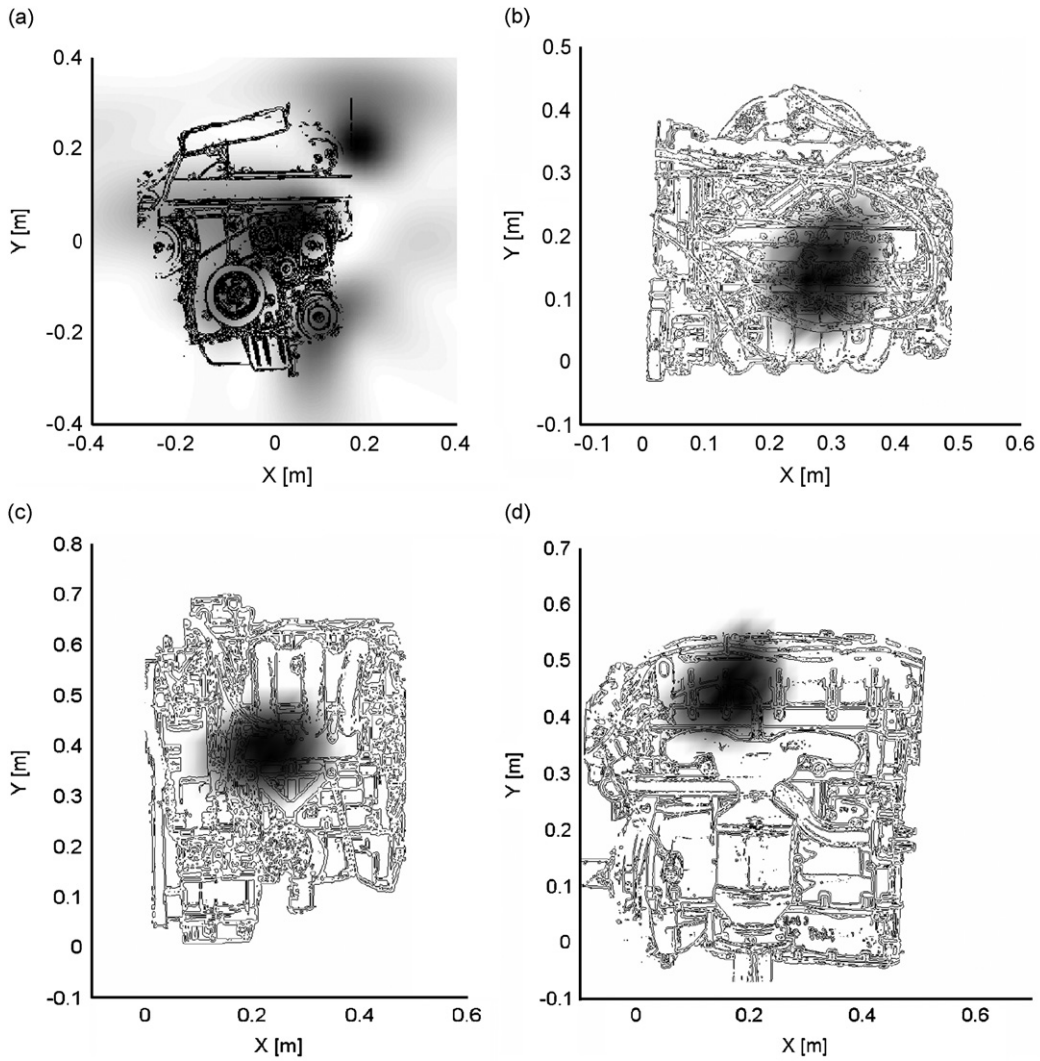
Fig. 9. Experimental results using the proposed method: (a) front side, (b) upper side, (c) right-hand side, and (d) left-hand side of the engine.

Acknowledgment

Appendix A. Noise modeling

The noise terms $n_1(t)$ and $n_2(t)$ are assumed to be mutually uncorrelated with each other and with $u(t)$ and $v(t)$. Assume that $u(t)$ and $v(t)$ are true signals from the measured $p_1(t)$ and $p_2(t)$, respectively. In this paper, $u(t)$ is $h(t)\delta(t-\tau_1)$ and $v(t)$ is $h(t)\delta(t-\tau_2)$, so the transfer function $T(\omega)$ becomes $e^{j\omega(d/c)\sin\theta_s}$ (see Fig. A1)

$$p_1(t) = u(t) + n_1(t), \quad p_2(t) = v(t) + n_2(t). \tag{A.1}$$

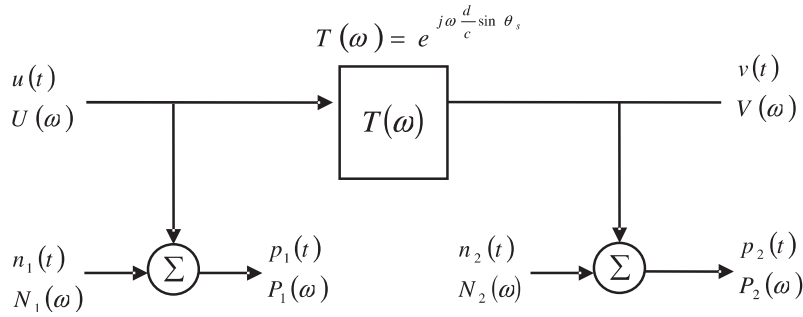$$T(\omega) = e^{j\omega \frac{d}{c} \sin \theta_s}$$

Fig. A1. One input/one output system with input and output noise.

The Fourier transform of $p_1(t)$ and $p_2(t)$ lead to

$$P_1(\omega) = U(\omega) + N_1(\omega), \quad P_2(\omega) = V(\omega) + N_2(\omega). \tag{A.2}$$

The measured cross-spectrum between $P_1(\omega)$ and $P_2(\omega)$ leads to

$$P_2(\omega)P_1^*(\omega) = \{V(\omega) + N_2(\omega)\}\{U(\omega) + N_1(\omega)\}^* = V(\omega)U^*(\omega) + A(\omega)$$
$$= T(\omega)U(\omega)U^*(\omega) + A(\omega) = T(\omega)\{P_1(\omega) - N_1(\omega)\}\{P_1(\omega) - N_1(\omega)\}^* + A(\omega), \tag{A.3}$$

where $A(\omega)$ is

$$A(\omega) = V(\omega)N_1^*(\omega) + U^*(\omega)N_2(\omega) + N_1^*(\omega)N_2(\omega). \tag{A.4}$$

Eq. (A.3) is divided by $P_1(\omega)P_1^*(\omega)$ which leads to the transfer function between $P_1(\omega)$ and $P_2(\omega)$

$$\frac{P_2(\omega)}{P_1(\omega)} = T(\omega) + \frac{T(\omega)}{P_1(\omega)P_1^*(\omega)}\{N_1(\omega)N_1^*(\omega) - P_1^*(\omega)N_1(\omega) - P_1(\omega)N_1^*(\omega)\} + \frac{A(\omega)}{P_1(\omega)P_1^*(\omega)}$$
$$= T(\omega) - \frac{T(\omega)}{P_1(\omega)P_1^*(\omega)}\{N_1^*(\omega)N_1(\omega) + U^*(\omega)N_1(\omega) + U(\omega)N_1^*(\omega)\} + \frac{A(\omega)}{P_1(\omega)P_1^*(\omega)}. \tag{A.5}$$

Because $n_1(t)$ and $n_2(t)$ are uncorrelated with each other and with $u(t)$ and $v(t)$, the second and third terms of the right-hand side of Eq. (A.5) can be assumed to be a noise with a continuous spectrum. That is, Eq. (A.5) can be simply express as

$$\frac{P_1(\omega)}{P_2(\omega)} = T(\omega) + N(\omega) = e^{j\omega(d/c)\sin \theta_s} + N(\omega). \tag{A.6}$$

References

[1] P.D. Mc Fadden, J.D. Smith, Model for the vibration produced by a single point defect in a rolling element bearing, *Journal of Sound and Vibration* 96 (1984) 69–82.

[2] S.K. Lee, P.R. White, The enhancement of impulsive noise and vibration signals for fault detection in rotating and reciprocating machinery, *Journal of Sound and Vibration* 217 (3) (1998) 485–505.

[3] Y.-H. Kim, B.-D. Lim, W.-S. Cheoung, Fault detection in a ball bearing system using a moving window, *Mechanical Systems and Signal Processing* 5 (1991) 461–473.

[4] W.J. Staszewski, G.R. Tomlinson, Local tooth fault detection in gearboxes using moving window procedure, *Mechanical Systems and Signal Processing* 11 (3) (1997) 331–350.

[5] E.R. Robinson, A.H. Quazi, Effect of sound-speed profile on differential time-delay estimation, *Journal of the Acoustical Society of America* 77 (3) (1985) 1086–1090.

[6] A.H. Quazi, An overview on the time delay estimate in active and passive systems for target localization, *IEEE Transactions on Acoustics, Speech, and Signal Processing* ASSP-29 (3) (1981).

[7] H.A. Canistraro, E.H. Jordan, Projectile-impact-location determination: an acoustic triangulation method, *Measurement Science & Technology* 7 (1996) 1755–1760.

[8] D.H. Johnson, D.E. Dudgeon, *Array Signal Processing*, PTR Prentice-Hall, Englewood Cliffs, NJ, 1993.

[9] J.-W. Choi, Y.-H. Kim, Estimation of locations and strengths of broadband planar and spherical noise sources using coherent signal subspace, *Journal of the Acoustical Society of America* 98 (4) (1995) 2082–2093.

[10] J.D. Maynard, E.G. Williams, Y. Lee, Nearfield acoustic holography: I. Theory of generalized holography and development of NAH, *Journal of the Acoustical Society of America* 78 (1985) 1395–1413.

[11] J. Capon, High-resolution frequency-wavenumber spectrum analysis, *Proceedings of the IEEE* 57 (8) (1969) 1408–1419.

[12] P.J. Sherman, On the family of the ML spectral estimates for mixed spectrum identification, *IEEE Transactions on Signal Processing* 39 (3) (1991) 644–665.

[13] D.E. Lyon, P.J. Sherman, Practical issues concerning the family of multichannel MV spectra for recovery of point spectrum, *IEEE Transactions on Signal Processing* 41 (11) (1993) 3177–3182.

[14] Y.-C. Choi, Y.-H. Kim, Detection of impulse signal in noise using a minimum variance cepstrum-application on faults detection in a bearing system, *Korean Society for Noise and Vibration Engineering* 10 (6) (2000) 985–990.

[15] M.H. Hayes, *Statistical Digital Signal Processing and Modeling*, Wiley, New York, 1996, pp. 426–433.

[16] International Organisation for Standardization, Draft Addendum ISO 3891/DAD 1, Acoustics, 1981.

[17] R.A. Horn, C.R. Johnson, *Matrix Analysis*, Cambridge University Press, Cambridge, 1985.

[18] A. Dancer, P. Grateau, Effectiveness of earplugs in high-intensity impulse noise, *Journal of the Acoustical Society of America* 91 (3) (1992) 1677–1689.

[19] G.R. Price, H.N. Kim, D.J. Lim, D. Dunn, Hazard from weapons impulses: histological and electrophysiological evidence, *Journal of the Acoustical Society of America* 85 (3) (1989) 1245–1254.

[20] P.D. Schomer, Growth function for human response to large-amplitude impulse noise, *Journal of the Acoustical Society of America* 64 (6) (1978) 1627–1632.

[21] R.P. Hamernik, K.D. Hsueh, Impulse noise: some definition, physical acoustics and other considerations, *Journal of the Acoustical Society of America* 90 (1) (1991) 189–196.

[22] R.R.A. Coles, G.R. Garinther, C.G. Rice, Hazardous exposure to impulse noise, *Journal of the Acoustical Society of America* 43 (2) (1968) 336–343.

[23] D. Henderson, R.P. Hamernik, Impulse noise: critical review, *Journal of the Acoustical Society of America* 80 (2) (1986) 569–584.

[24] S. Raghunathan, H.D. Kim, T. Setoguchi, Impulse noise and its control, *Progress in Aerospace Science* 34 (1998) 1–44.